Energy & Environmental Science

Systematic over-estimation of lattice thermal conductivity in materials with electrically-resistive grain boundaries

Journal:	*Energy & Environmental Science*
Manuscript ID	EE-ART-12-2019-003921.R1
Article Type:	Paper
Date Submitted by the Author:	14-Feb-2020
Complete List of Authors:	Kuo, Jimmy; Northwestern University, Wood, Max; Northwestern University, Materials Science and Engineering Slade, Tyler; Northwestern University, Chemistry Kanatzidis, Mercouri; Northwestern University, Department of Chemistry Snyder, G.; Northwestern University, Materials Science

Systematic over-estimation of lattice thermal conductivity in materials with electrically-resistive grain boundaries

Jimmy Jiahong Kuo, Max Wood, Tyler J. Slade, Mercouri G. Kanatzidis, and G. Jeffrey Snyder*

Northwestern University, Evanston, IL 60208, USA

E-mail: jeff.snyder@northwestern.edu

Abstract

Reducing the thermal conductivity κ of a material via nano-structuring to create small grain sizes is one of the most common strategies to improve thermoelectric materials. In such polycrystalline materials heat carrying phonons are scattered at the grain boundaries, which directly improves the thermoelectric quality factor and ultimately the figure-of-merit zT. In some cases, however, such as in Mg_3Sb_2, SnSe, and Mg_2Si an opposite trend is found where higher lattice thermal conductivity reported in small grain polycrystalline material than in large grain or single crystal materials. This unphysical result indicates a problem with the conventional use of the Wiedemann-Franz law. Here, we trace this problematic finding to the electrical resistance at the grain boundaries, which leads to an overestimation of the phonon or lattice contribution to the thermal conductivity κ_L. In materials with significant grain boundary electrical resistance, the estimated electronic contribution to the thermal conductivity $L\sigma T$ is low because the measured electrical conductivity σ is low. However within the grain electrons may still be transporting more heat than the total conductivity suggests,

leading to an overestimation of κ_L if the conventional $\kappa_L = \kappa - L\sigma T$ is used with the measured values of κ and σ. The overestimation of κ_L in small-grain samples is shown to be pervasive across a broad range of thermoelectric materials, including Mg_3Sb_2, Mg_2Si, PbTe, PbSe, SnSe, (Hf,Zr)CoSb, $CoSb_3$, and Bi_2Te_3 alloys, and a correction is necessary to properly understand and predict their charge and heat transport.

Introduction

Engineering materials to achieve lower κ_L is receiving growing attention due to their importance in thermoelectric applications.[1] One common method to achieve this is via introducing nano-structures at grain boundaries which enhances the scattering rate of phonons.[2,3] In general, grain boundaries can scatter not only heat carriers but also charge carriers. A correlation between the electrical mobility and the average grain size has been reported in various thermoelectric materials, such as Mg_3Sb_2,[4,5] Mg_2Si,[6,7] (Hf, Zr)CoSb,[8] NbFeSb,[9] SnSe,[10] PbSe[11] etc. Electrons and phonons are not necessarily scattered by grain boundaries at similar strengths, leading to a strategy of grain boundary engineering where engineers can optimize the thermoelectric performance by changing the average grain size.

Normally, with increasing density of grain boundaries the scattering rates of electrons and phonons are expected to both be higher. This relationship predicts the κ_L and electrical weighted mobility μ_W[12–14] of a series of different grain sized samples at the same temperature to be directly correlated. Alloys of Silicon-Germanium (Si-Ge), in which the properties of nano-structured samples have been widely studied for thermoelectric applications, show this expected trend of decreasing κ_L and decreasing μ_W as the grain size is reduced for both n-type and p-type samples[15] (Fig. 1(a)).

However, in some of the aforementioned examples an unphysical inverse correlation between κ_L and μ_W was observed.[4,6,11] The new high-zT n-type Mg_3Sb_2-Mg_3Bi_2 alloys,[4,16] for example (Fig. 1(b)), show the expected decrease in μ_W (at low temperatures) when the average grain size decreases. However, in contrast, κ_L shows an unexpected increasing trend with

decreasing grain size, which appears contradictory to the standard grain-boundary scattering theory for phonons. At higher temperatures (*e.g.* 573 K), the scattering of electrons at grain boundaries becomes less significant,[5] which leads to similar μ_{W} among samples. At the same time, the discrepancy of κ_{L} between samples goes away, suggesting that these properties are somehow related through the electrical grain-boundary effect. These opposite trends in the κ_{L}-μ_{W} relationship offers a simple way to identify if this unusual behavior is occurring even without a measurement of grain size.

In the above examples, the conventional method of calculating κ_{L} relies on the Wiedemann-Franz law, in which the thermal conductivity arising from charge carriers is subtracted out from the measured total thermal conductivity to estimate the lattice contribution to thermal conductivity:

$$\kappa_{\mathrm{L}} = \kappa_{\mathrm{total}} - L\sigma T. \tag{1}$$

The unexpectedly high κ_{L} was often explained by an underestimation of the electronic contribution to the thermal conductivity κ_{e} ($L\sigma T$). However the origins of this overestimation were either unexplained or sometimes corrected using an unphysically large Lorenz number.[6,17]

An often overlooked assumption needed when in using the Wiedemann-Franz law is that the Lorenz number and electrical conductivity used to calculate the electron contribution to thermal conductivity are for a homogeneous material where the scattering probability is assumed to be uniform everywhere. In a homogeneous material the individual contribution to heat transport from electrons and phonons can be well-defined. However, this assumption can break down for an inhomogeneous material, when the length scale of the heterogeneity is larger than the mean-free-path or the coherence length. Inhomogeneity is common in thermoelectric materials at small length scales (point defects) but also at large length scales such as dislocations, secondary phases (*e.g.* nano-composite[18]) and grain boundaries[19]), which can lead to a break down of the conventional model. In these cases, the heat can transfer from electrons to phonons and one phase to the next depending on how the phases are interconnected, which could be modeled, for example, via an effective-medium theory.

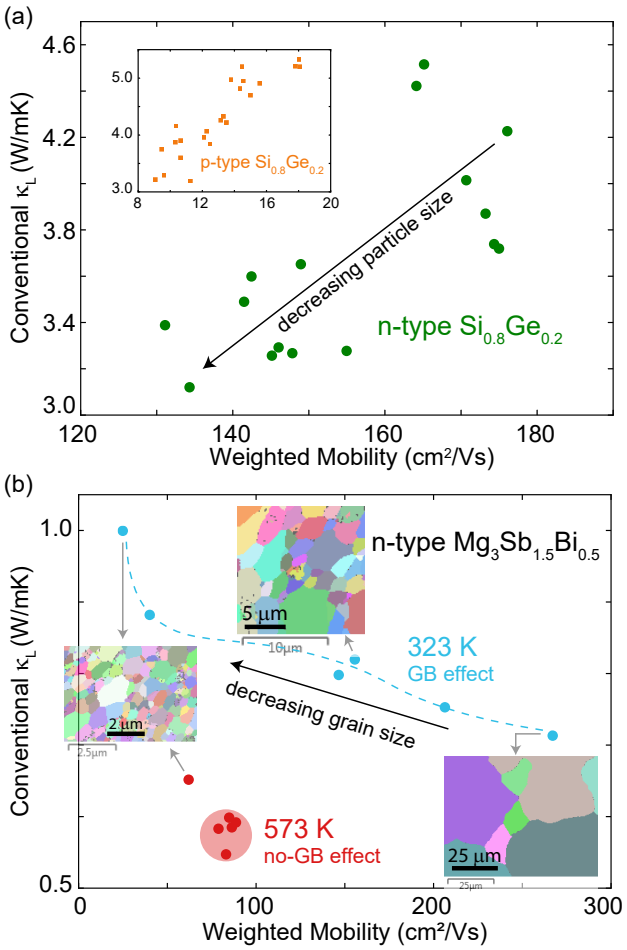

Figure 1: Lattice thermal conductivity as conventionally calculated $\kappa_L(\kappa_{total} - L\sigma T)$ vs weighted mobility μ_W[12,14](see SI for the derivation) of SiGe alloy and Mg_3Sb_2 samples with different average particle/grain sizes. (a) Both n-type (P-doped) and p-type (B-doped) SiGe show a positive correlation at room temperature. (b) For Mg_3Sb_2 at high temperatures (573K) electrons are not significantly scattered by grain boundaries and the weighted mobility is the same except for the smallest grain size sample. In contrast, at low temperatures (323K) μ_W decreases significantly as grain size is decreased, making low μ_W a good indicator of grain boundary electrical resistance. The trend of increasing κ_L with decreasing μ_W indicates a grain boundary effect even without measurement of grain size.

Herein we show the apparent increase in lattice thermal conductivity with decreasing grain size is not from a true increase in the phonon contribution to thermal conductivity, but instead an artifact of assuming homogeneous electron and phonon transport in a material. We apply a correction to the conventional model to calculate the κ_L. We provide a theoretical argument and experimental evidence to show that treating grain boundary regions as a second phase is essential to obtain a correct κ_L of the material. In particular, the

correction can be significant in materials with high weighted mobility and low total thermal conductivity, therefore making this crucial in many high-zT thermoelectric materials. A proper calculation of κ_{L} is essential for a quality factor analysis (to estimate the maximum thermoelectric figure-of-merit zT[12,14]), as well as in phonon-scattering models (to quantify the contribution of each scattering mechanism). The unphysical inverse relationship between mobility and apparent lattice thermal conductivity calculated conventionally is widespread throughout the literature and was previously unexplained or incorrectly diagnosed as an exotic Lorenz number phenomenon.

Breakdown of the homogeneous picture

Conventionally, charge and heat transport in solids are often modeled via constructing a relaxation time τ which is combined with other scattering mechanisms probabilistically using Matthiessen's rule (*i.e.* $\tau^{-1} = \sum \tau_i^{-1}$). Two assumptions behind this model are (1) the carrier mean free path is much larger than the scale of the scattering centers and (2) the probability of scattering from each mechanism is independent of each other.[20] Using this probabilistic model, the material as a whole is considered homogeneous, even with multiple types of defects present. As a result, the two transport channels of heat, through charge carriers (*e.g.* electrons or holes) and through lattice vibrations (*e.g.* phonons, diffusons, etc.), have no spatial variation across the entire system and are effectively independent. This validates the conventional thermal conduction equation in which the total thermal conductivity is the summation of contribution from each channel (Eq. 1).

In polycrystalline Mg_3Sb_2-based compounds, however, we find evidence that this homogeneous picture is not appropriate to model the effect of grain boundaries on charge transport. Using atom-probe tomography, we measured the width of local Mg deficiency across grain boundaries to be $\approx$ 10 nm in Mg_3Sb_2.[21] This off-stoichiometry can induce a charged potential barrier wider than 10 nm, which is larger than the estimated electron mean free

path (≈ 8 nm). This inhomogeneity violates our first assumption in Matthiessen's rule, and necessitates a two-phase model to describe charge transport.[5]

In the following sections, we demonstrate how a two-phase model leads to a fundamentally different picture of heat transport, which corrects the decreasing trend of κ_L shown in Fig. 4. We propose that materials with similar μ_W-κ_L trend as Mg_3Sb_2 would benefit from an analysis using the two-phase model to correctly estimate the lattice thermal conductivity and would be necessary to understand and engineer their thermoeletric properties.

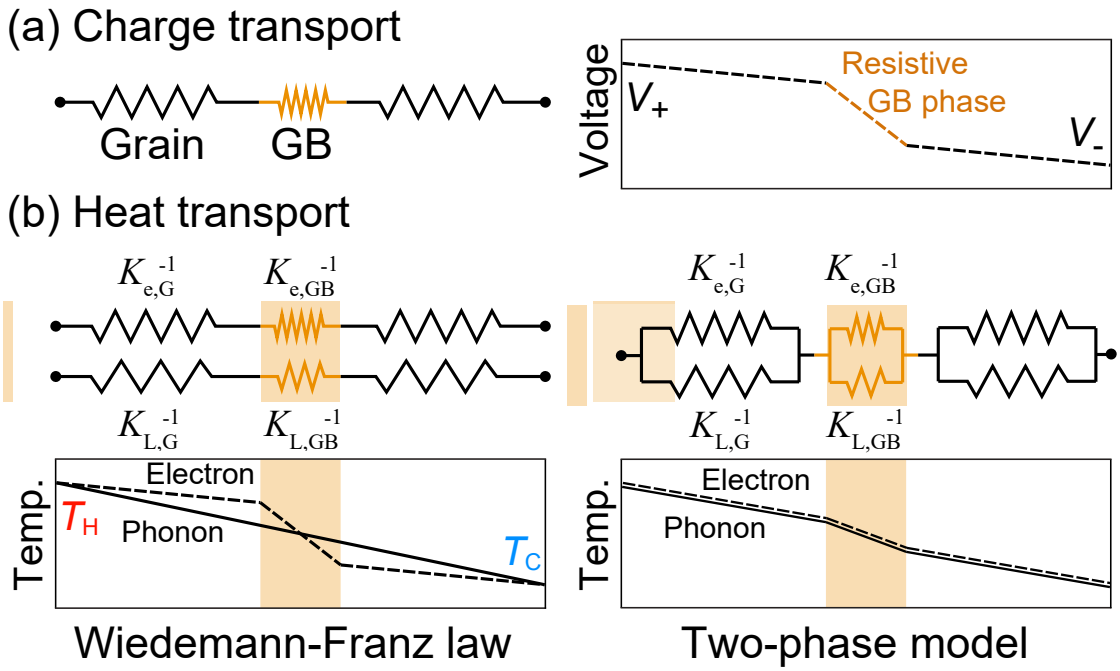

Figure 2: Equivalent circuits for treating thermal and electrical resistance of grain boundaries. The charge and heat transport is approximated as a 1-D series circuit because the grain-boundary phase (GB) is very thin and more resistive compared to the grain phase (G). The voltage profile across a grain boundary is shown, in which a significant portion of voltage drop is from the grain-boundary phase. Whereas only electrons transport charge (one channel transport, see (a)), both electrons (e) and phonons (L) contribute to heat transport (two channel transport of heat, see (b)). The "conventional Wiedemann-Franz law" (Eq 1) is tantamount to assuming these two channels are completely isolated and all the heat transported by electrons in a grain (through $(1/K_{e,G})$) must also be transported by electrons in the grain boundary, $(1/K_{e,GB})$. In the two-phase model, the heat transported by electrons in the grain can switch to the lower resistance lattice thermal conduction path within the grain boundary, $(1/K_{L,GB})$. For a material with inhomogeneity due to nano-structures, applying the conventional model falsely results in different temperature profiles between the two channels, whereas the two-phase model avoids the problem.

The two-phase model

Thermodynamically, grain boundaries can demonstrate phase-like properties which are referred to as grain-boundary complexions.[22] For charge and heat transport, treating the boundary as a phase implies it has its own unique transport properties (*e.g.* electrical & thermal conductivity and Seebeck coefficient) which can be different from those of the bulk phase. When multiple phases co-exist in a compound, an effective-medium approach[23,24] should be considered to model the total transport properties considering the configuration of the phases.

In Mg_3Sb_2-based compounds, because the boundaries are more electrically resistive than the bulk, the equivalent charge conduction can be approximated as a one-dimensional series circuit[5] (Fig. 2(a)). For heat transport, the conventional use of the Wiedemann-Franz Law (Eq. 1) effectively treats the heat transported by phonons (the lattice thermal conductivity due to atomic vibrations in a solid) and charge carriers as two independent, parallel transport channels of heat (Fig. 2(b)-left). A consequence of this assumption is that the heat energy carried through the electron channel cannot be transferred to the phonon channel. Microscopically, this requires no net exchange of energy between electrons and phonons at grain boundaries or anywhere else. Such a model is incorrect, because it states that an electrically-insulating layer or surface can prevent charge carriers from contributing to heat conduction. This in turn leads to a vastly different temperature distribution for electrons and phonons which is unphysical. An intuitive example of this is that simply wrapping an insulating sheet of paper on a metal block will not eliminate the heat transported by the free electrons inside. Based on these arguments, we propose a correction of the equivalent thermal conduction circuit (Fig. 2(b)-right). The concept behind this circuit is to treat the grain boundaries as a separate phase, containing its own heat transport channels (in parallel) connected with those of the bulk in a series-circuit manner. In this model the temperature profile along the electron and phonon channels are the same.

Heat transport dominated by bulk grains

A polycrystalline sample's heat transport is approximately dominated by the bulk media of the grain when the length of the grain-boundary is orders of magnitude thinner than that of the bulk. In the series-circuit model, the total thermal resistance is equal to the summation of individual resistances: $K_{\text{total}}^{-1} = K_{\text{G}}^{-1} + K_{\text{GB}}^{-1}$ (G for bulk grain and GB for grain boundary). The thermal resistance can be formulated by Fourier's Law: $K^{-1} = \kappa^{-1}\ell/A = (\kappa_{\text{L}} + \kappa_{\text{e}})^{-1}\,\ell/A$, where ℓ and A are length and area of the resistor. Due to the relatively thin width of the grain-boundary phase compared to the bulk (*e.g.* $\ell_{\text{GB}}/\ell_{\text{G}} \approx 10^{-3}$ in Mg_3Sb_2 [21]) we neglect the thermal resistance of the grain boundary (see Sec. S2 in the SI for explanation of the discrepancy between charge and heat transport). Under this approximation, the lattice thermal conductivity is dominated by the bulk, which can be calculated via

$$\kappa_{\text{L}} \approx \kappa_{\text{L,G}} = \kappa - L\sigma_{\text{G}}T, \tag{2}$$

where σ_{G} is the conductivity of the bulk grain rather than the total conductivity as used in the conventional model.

Tuning the electron thermal conductivity in Mg_3Sb_2

The case study of Mg_3Sb_2 provides a way to compare the κ_{L} of a single sample with and without the charge transport channel. Mg_3Sb_2 is chosen because the charge carrier concentration of the compound can be controlled via a short saturation anneal (*e.g.* 1 hour) in Mg vapor. Before annealing there are few free electrons and the thermal conductivity is dominated by phonons like in an insulator. After annealing with Mg vapor the material has many free electrons like a metal. Shown in Fig. 3(a), a Mg-deficient, Te-doped $Mg_{3-\delta}Sb_{1.5}Bi_{0.49}Te_{0.01}$ sample was prepared, with a low electrical conductivity, and a non-degenerate Hall carrier concentration due to the formation of Mg vacancies that act as electron-killer defects (V_{Mg}^{2-}).[4]

The thermal conductivity of this electrically insulating sample was measured to obtain its true lattice thermal conductivity. After this, the sample was annealed in Mg vapor for 1 hour, which increased the sample's carrier concentration and conductivity (Fig. 3(b)) by orders of magnitude. The geometrical density remains unchanged within expiramental error after the anneal (4.52±0.05 g/cm^3). We then measured the thermal conductivity of this sample again, now with its charge transport channel activated. The thermally-activated electrical conductivity along with a temperature independent carrier concentration demonstrates that the grain-boundary effect is still in affect at low temperatures, compared to the predicted no-grain-boundary limit extrapolated from high-temperature data (black line in Fig. 3(b)).

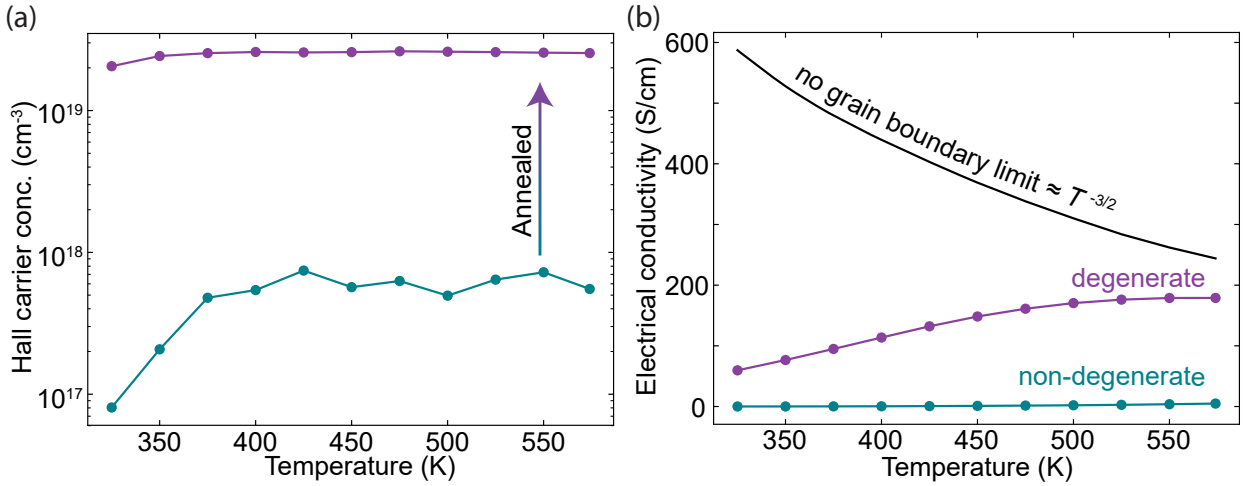

Figure 3: Temperature dependence of Hall carrier concentration and conductivity of Te-doped Mg_3Sb_2 (nominal composition: $Mg_{3-\delta}Sb_{1.5}Bi_{0.49}Te_{0.01}$) before (cyan color) and after (purple color) annealed in Mg vapor. (a) The Hall carrier concentration is initially intrinsic-semiconductor-like (increasing with temperature) and then becomes metal-like (constant with temperature). (b) Due to the enhanced free-carrier concentration after annealing, the electrical conductivity also increased. The thermally-activated conductivity is due to grain boundary scattering of electrons, which is eliminated at higher temperatures. An estimate of bulk conductivity (black solid line) can be calculated using weighted mobility from the larger grain-size data published previously[25] (see Sec. S1 in the SI).

Comparisons between κ_L before and after annealing verifies the two-phase model. Before annealing the electrical conductivity is almost zero and therefore the measured κ_{total} (Fig. 4) should only be the lattice contribution κ_L with a possible small bipolar contriubtion at higher temperatures. After annealing, the contribution of heat conduction from charge carriers is

significant. Treating the non-degenerate case (cyan color) as a reference, the conventional model overestimates $\kappa_{\mathrm{L,\ conv.}}$ near room temperature, and slowly converges to the reference as the temperature increases. Conversly, using the no-grain-boundary limit of electrical conductivity (calculated based on the large grain-size sample,[16] see Sec. S1 in the SI), κ_{L} calculated from the two-phase model is consistent with the non-degenerate values. The $\approx 8\%$ discrepancy at high temperature is likely due to bipolar effect in the non-degenerate sample.

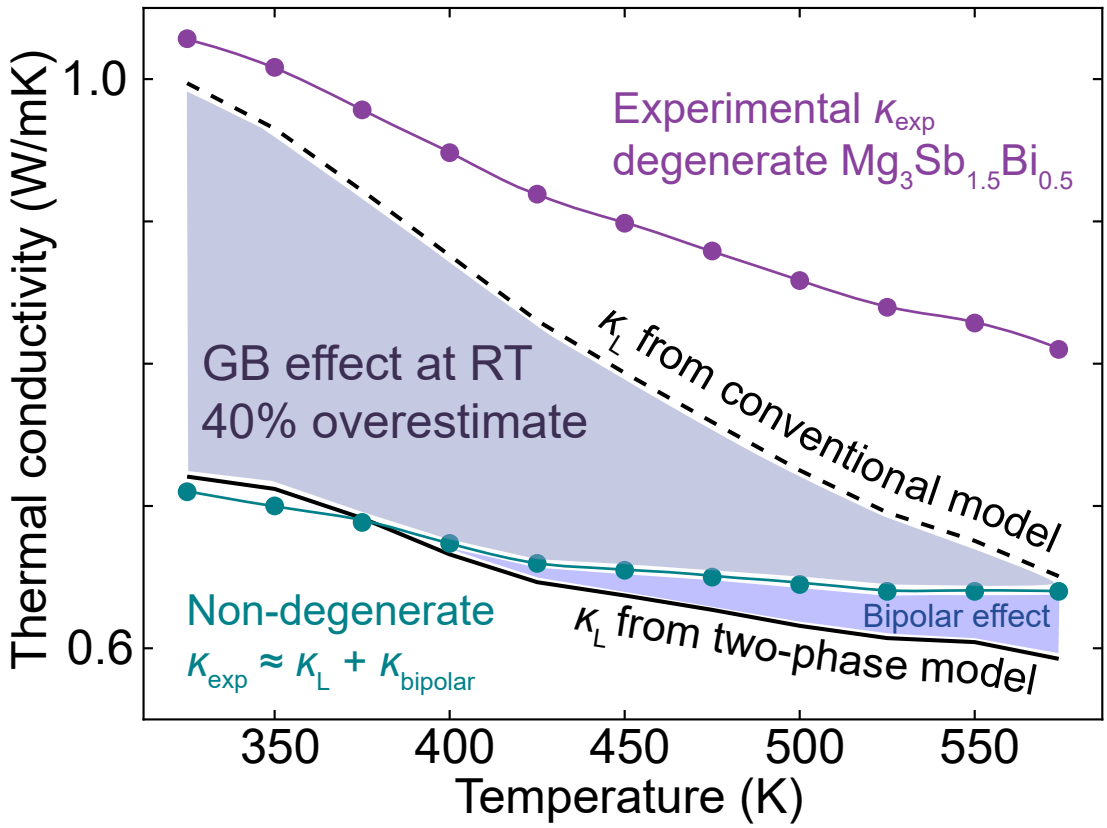

Figure 4: Temperature dependant thermal conductivity of $Mg_{3-\delta}Sb_{1.5}Bi_{0.49}Te_{0.01}$) before (blue dots) and after (purple dots) being injected with carriers via a Mg vapor anneal. The blue dots show the material's thermal conductivity when its electrical conductivity is negligibly small, thus giving an experimental lattice thermal conductivity. The grey dashed line shows the overestimated conventional lattice thermal conductivity calculated from the electrically conducting sample (red data). The two phase model (solid black line) considers the effect of electrical grain boundary resistance, and is in better agreement with true lattice thermal conductivity except for the high temperature which can be due to bipolar effect in the non-degenerate sample.

The two-phase model can be applied to compare with the inverse correlation between

conventional lattice thermal conductivity and weighted mobility observed from Mg_3Sb_2 (Fig. 1(b)). Fig. 5 shows how the conventional model (Eq. 1) generally calculates larger κ_L for small-grain samples, whereas the two-phase model gives similar value for all the cases. Qualitatively, our model solve the inconsistency between the conventional κ_L model and the phonon scattering theory mentioned in the Introduction.

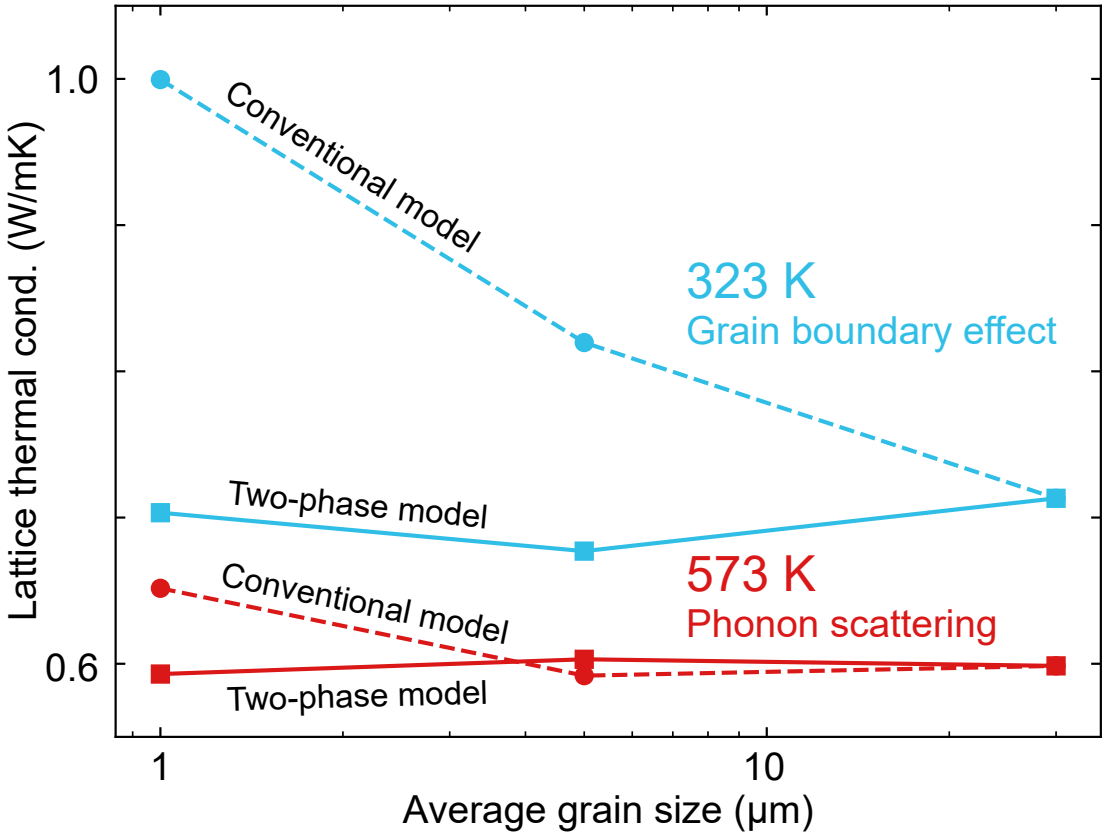

Figure 5: Comparison of models for lattice thermal conductivity in materials with different grain sizes. The conventional model (dash lines) gives higher κ_L for small-grain sample at both 323 K (bule) and 573 K (red). In contrast, the two-phase model (solid lines) give similar κ_L. Note that the bulk conductivity of all samples are estimated by using the weighted mobility of the large-grain sample with $\approx 30\mu$m (see Sec. S1 in the SI).

Broader Applicability

As thermoelectric applications require a material to have high electrical mobility and low lattice thermal conductivity, the charge-carrier contribution to heat transport is generally

similar in magnitude to the lattice contribution. As a result, significant corrections of κ_L should be expected in various other high-zT thermoelectric materials where electronic grain boundary scattering is present.

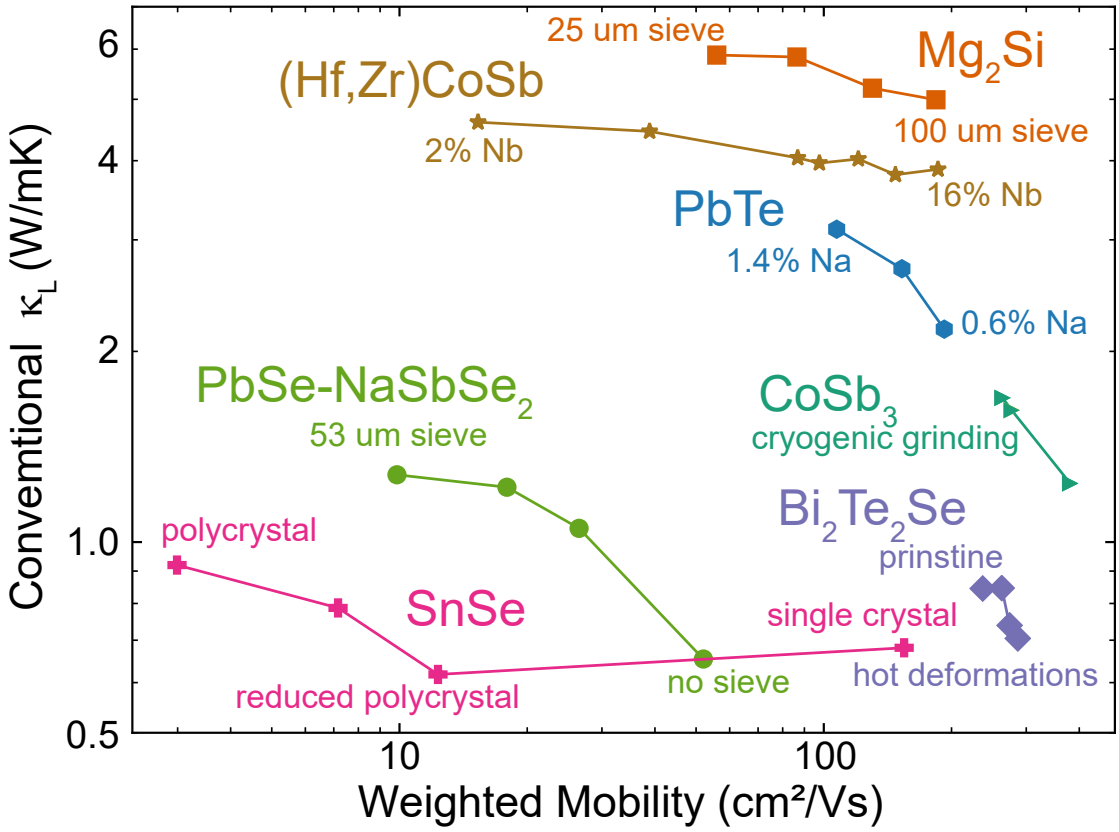

Figure 6: Weighted mobility vs conventional lattice thermal conductivity (Eq.1) plot at 350 K. The plot resembles Fig. 1 and a negative slope serves as a indicator that κ_L may require correction. Data described in the text includes Mg_2Si,[7] (Hf,Zr)CoSb,[8] PbTe,[26] PbSe alloy,[11,27] SnSe,[28,29] $CoSb_3$,[30] and Bi_2Te_2Se.[31]

Once again we point out the counterintuitive result that various thermoelectric systems have their mobilities and reported lattice thermal conductivities inversely correlated in contrast to the Si-Ge result of Fig. 1(a). This correlation is explained for the first time, suggesting a correction for κ_L is required, and is evidence that our model is system independent.

Fig. 6 includes materials synthesized with different grain sizes (Mg_2Si,[7] PbSe alloys,[11,27] and SnSe[29,32]), and those processed without specifically targeting their grain-boundary properties but showing a similar trend as Mg_3Sb_2 (PbTe, (Hf,Zr)CoSb,[8] $CoSb_3$,[30] and

Bi_2Te_2Se[31]). The following sections summarizes the details of each system and the impact of their processing method on the reported lattice thermal conductivity. Complete data of μ_W and κ_L can be found in Sec. S4 in the SI.

Mg_2Si & PbSe

The grain-boundary effect in Mg_2Si was first identified by J. De Boor et al., who associated the thermally-activated conductivity with the amount of MgO segregation at grain boundaries.[7] In the follow-up work,[6] a comparison between different sieved-size powers and the electrical conductivity further confirmed the grain-boundary effect. Fig. 6 shows that sieving reduced the μ_W, which can be due to the increased grain-boundary density. The increased $\kappa_{L,\,conv.}$, is explained by a Lorenz-factor argument, but instead could be due to the grain boundary effects describe here requiring a κ_L correction. A similar observation can be seen from the PbSe-$NaSbSe_2$ alloy system, in which samples prepared with larger grains have apparently smaller κ_L than small grain samples.[11] We will discuss the GB effect in these PbSe-$NaSbSe_2$ alloys in greater detail an upcoming manuscript.[27]

SnSe: single/polycrystal & H_2 reduction

Polycrystalline SnSe suffers from grain boundary resistance, which is evident from its thermally activated mobility that single crystal samples do not display.[33] While measurements of the thermal conductivity in single crystals vary[32,34–37] some are lower than that reported for polycrystalline material. Given this context, grain boundary resistance could be a contributing factor into why the conventional lattice thermal conductivity in polycrystalline samples of SnSe could be higher than that of a single crystal. Attempts to modify the oxygen content in grain boundaries of SnSe[29] found that the apparent lattice thermal conductivity could be reduced by the reduction of SnO in the grain boundaries. While this has been attributed to high thermal conductivity of SnO we suspect the grain boundary resistance is also having an effect as evidenced by the large increase in the mobility observed. This would mean the

lattice thermal conductivity was simply overestimated in samples with SnO at the grain boundaries due to the grain boundary resistance from the oxide layer.

PbTe: Dopant Solubility Exceeded

A grain-boundary effect in K,Na co-doped PbTe, may also have been observed when the solubility of their dopant was exceeded.[26] At temperatures above 500K co-doped samples follow the normal lattice thermal conductivity of pure PbTe reasonably well. However at temperatures bellow 500K, samples that have K = 1.25 % and Na > 0.8 % had lattice thermal conductivities that were higher than that of pure PbTe. Additionally, these high lattice thermal conductivity samples had almost identical Seebeck values, suggesting the solubility limit of the dopant had been reached. An anomalous Lorenz number was proposed to be due to interband scattering, which increases the Lorenz number beyond the degenerate limit. The two-phase grain-boundary model provides a simpler explanation. After the solubility limit of the dopant is reached, additional dopant atoms segregate to the grain boundary forming an electrically resistive grain boundary phase. As more dopant is added the amount of this phase increases, lowering the composite material's mobility, while increasing it's conventional lattice thermal conductivity.

Half Heusler

In (Hf,Zr)CoSb, an electrical grain-boundary effect was identified.[8] Doping with Nb, presumably altering the grain-boundary scattering potential barrier, improved the overall electrical mobility. Moreover, a reduction of κ_{L} was observed with increasing Nb content. We suspect that the lower κ_{L} can be a combined effect of disorder scattering (as claimed in the publication) and the grain boundary effect that leads to an overestimate of κ_{L}. The degree of each can be calculated by measuring κ_{L} of samples with larger grain sizes, as done in this study.

$CoSb_3$ Skutterudite

Cryogenic grinding of Yb-filled $CoSb_3$ powders was reported to lower κ_L due to a reduction of average grain sizes.[30] While the average grain size of the samples can be correlated with the duration of cryogenic grinding, extended grinding (*i.e.* 60 and 120 mins) shows an enhanced κ_L which has not yet been well-understood. It was also suspected that the significant reduction of electrical conductivity is associated with grain-boundary scattering, and the reported κ_L is more of an overestimation due to the underestimate κ_e.[30]

Bi_2Te_3-based materials

There have been several studies showing that as $Bi_2(Te,Se)_3$ is hot deformed, its thermoelectric properties are enhanced.[31,38,39] For example, hot deformation results in grain growth in n-type Bi_2Te_2Se with an increase in the material's mobility and decrease in the material's lattice thermal conductivity.[31] A lattice defect argument was used to explain the reduction of their samples' lattice thermal conductivity, but the authors did not show any direct evidence lattice defects were present in their samples. Additionally this argument does not explain why the weighted mobility is higher in samples with low reported lattice thermal conductivity. The grain boundary effect may give a physical reason why these parameters are so connected due to the reduction of grain boundary scattering from the grain growth witnessed during hot deformation.

The grain boundary electrical resistance explanation is further supported by a study that investigated the effect of ball milling time on grain size and the thermoelectric properties of n-type $Bi_2(Te,Se)_3$.[40] It was noted that the lattice thermal conductivity of the largest grained sample was lower than samples that were ball milled for longer times and had smaller grain sizes. Extracting a weighted mobility from the conductivity and Seebeck data, we can see that this large grained sample also had the largest weighted mobility and likely suffered the least from electrical grain boundary resistance.

Conclusion

We have demonstrated that an inhomogeneous, two-phase description is necessary to accurately calculate the lattice thermal conductivity of materials with grain-boundary scattering of charge carriers. We experimentally validated this model in Mg_3Sb_2 that we were able to test and compare its lattice thermal conductivity with and without the electronic contribution to the thermal conductivity. We showed several examples found in the literature that exhibit electronic grain boundary scattering where the apparent lattice thermal conductivity, calculated from $\kappa_L = \kappa - L\sigma T$ is overestimated affecting conclusions about nanostructuring or the Lorenz factor in the Wiedemann-Franz law that may be incorrect.

Methods

Sample preparation

We sealed magnesium turnings (99.98 %, Alfa Aesar), antimony shots (99.9999 %, 5N Plus), bismuth shots (99.9999 %, 5N Plus), and Te shot (99.999 %, 5N Plus) into stainless-steel vials according to stoichemetric ratios in an argon-filled glove box.The nominal composition we used for the magnesium deffecient sample tested in this study was $Mg_{2.95}Sb_{1.49}Bi_{0.5}Te_{0.01}$. Elements were mechanically alloyed by high energy-ball milling with a high-energy mill (SPEX 8000D) for two hours. The processed powder was loaded into a graphite die with half inch diameter and pressed by an induction heating rapid hot press[41] for 60 minutes at 873 K at 45 MPa under argon gas flow.

Annealing process

Hot-pressed pellets were placed into a magnesium oxide crucible (25 mm diameter, 25 mm height). Magnesium turnings (99.98 %, Alfa Aesar) are added such that both sides of the pellet are in contact with Mg turnings. The crucible was loaded into a graphite die and

covered by a piece of graphite foil and graphite spacer to create a quasi-isolating environment for the pellet. The graphite die was heated up by a induction heater to 873 K under argon gas flow.

Measurements of transport properties

Electrical and thermal transport properties were measured from 323 to 573 K. The electrical resistivity and Hall coefficient measurements were determined using the 4-point probe Van der Pauw technique with a 0.8 T magnetic field under high vacuum.[42] The Seebeck coefficients of the samples were obtained using chromel-Nb thermocouples by applying a temperature gradient across the sample to oscillate between ±5 K.[43] Thermal conductivity was calculated from the relation $\kappa = DdC_p$, where D is the thermal diffusivity measured with a Netzsch LFA 457 laser flash apparatus, d is the geometrical density of the material and C_p is the heat capacity at constant pressure. C_p the compounds were calculated via the polynomial equation proposed by Agne et al.[44]

Author contributions

J.J.K. and M.W. contributed equally to this work. J.J.K. and M.W. conceived the project and wrote the manuscript. J.J.K., M.W. and T.J.S. conducted the experiments. G.J.S. supervised the project. All authors edited the manuscript.

Acknowledgement

This research was carried out under a contract with the National Aeronautics and Space Administration and was supported by the NASA Science Mission Directorate's Radioisotope Power System Technology Advancement Program. J.J.K., M.W. and G.J.S. also gratefully acknowledge thermoelectrics research at Northwestern University through the Center for

Hierarchical Materials Design (CHiMaD). T.J.S. and M.G.K. acknowledge the support from U.S. Department of Energy, Office of Science and Office of Basic Energy Sciences under award number DE-SC0014520-0003.

References

(1) Snyder, G. J.; Toberer, E. S. *Materials For Sustainable Energy: A Collection of Peer-Reviewed Research and Review Articles from Nature Publishing Group*; World Scientific, 2011; pp 101–110.

(2) Wang, X. W.; Lee, H.; Lan, Y. C.; Zhu, G. H.; Joshi, G.; Wang, D. Z.; Yang, J.; Muto, A. J.; Tang, M. Y.; Klatsky, J.; Song, S.; Dresselhaus, M. S.; Chen, G.; Ren, Z. F. Enhanced thermoelectric figure of merit in nanostructured n-type silicon germanium bulk alloy. *Applied Physics Letters* **2008**, *93*, 193121.

(3) Zong, P.-a.; Hanus, R.; Dylla, M.; Tang, Y.; Liao, J.; Zhang, Q.; Snyder, G. J.; Chen, L. Skutterudite with graphene-modified grain-boundary complexion enhances zT enabling high-efficiency thermoelectric device. *Energy & Environmental Science* **2017**, *10*, 183–191.

(4) Kanno, T.; Tamaki, H.; Sato, H. K.; Kang, S. D.; Ohno, S.; Imasato, K.; Kuo, J. J.; Snyder, G. J.; Miyazaki, Y. Enhancement of average thermoelectric figure of merit by increasing the grain-size of $Mg_{3.2}Sb_{1.5}Bi_{0.49}Te_{0.01}$. *Applied Physics Letters* **2018**, *112*, 033903.

(5) Kuo, J. J.; Kang, S. D.; Imasato, K.; Tamaki, H.; Ohno, S.; Kanno, T.; Snyder, G. J. Grain boundary dominated charge transport in Mg_3Sb_2-based compounds. *Energy & Environmental Science* **2018**, *11*, 429–434.

(6) De Boor, J.; Compere, C.; Dasgupta, T.; Stiewe, C.; Kolb, H.; Schmitz, A.; Mueller, E.

Fabrication parameters for optimized thermoelectric Mg_2Si. *Journal of materials science* **2014**, *49*, 3196–3204.

(7) de Boor, J.; Dasgupta, T.; Kolb, H.; Compere, C.; Kelm, K.; Mueller, E. Microstructural effects on thermoelectric efficiency: A case study on magnesium silicide. *Acta Materialia* **2014**, *77*, 68–75.

(8) Qiu, Q.; Liu, Y.; Xia, K.; Fang, T.; Yu, J.; Zhao, X.; Zhu, T. Grain Boundary Scattering of Charge Transport in n-Type (Hf, Zr) CoSb Half-Heusler Thermoelectric Materials. *Advanced Energy Materials* **2019**, *9*, 1803447.

(9) He, R.; Kraemer, D.; Mao, J.; Zeng, L.; Jie, Q.; Lan, Y.; Li, C.; Shuai, J.; Kim, H. S.; Liu, Y.; Broido, D.; Chu, C.-W.; Chen, G.; Ren, Z. Achieving high power factor and output power density in p-type half-Heuslers $Nb_{1-x}Ti_xFeSb$. *Proceedings of the National Academy of Sciences* **2016**, *113*, 13576–13581.

(10) Wei, T.-R.; Tan, G.; Zhang, X.; Wu, C.-F.; Li, J.-F.; Dravid, V. P.; Snyder, G. J.; Kanatzidis, M. G. Distinct Impact of Alkali-Ion Doping on Electrical Transport Properties of Thermoelectric p-Type Polycrystalline SnSe. *Journal of the American Chemical Society* **2016**, *138*, 8875–8882.

(11) Slade, T. J.; Bailey, T. P.; Grovogui, J. A.; Hua, X.; Zhang, X.; Kuo, J. J.; Hadar, I.; Snyder, G. J.; Wolverton, C.; Dravid, V. P.; Uher, C.; Kanatzidis, M. G. High Thermoelectric Performance in PbSe–$NaSbSe_2$ Alloys from Valence Band Convergence and Low Thermal Conductivity. *Advanced Energy Materials* **2019**, 1901377.

(12) Wang, H.; Pei, Y.; LaLonde, A. D.; Snyder, G. J. *Thermoelectric Nanomaterials*; Springer, 2013; pp 3–32.

(13) May, A. F.; Snyder, G. J. *Materials, preparation, and characterization in thermoelectrics*; CRC Press, 2017; pp 11–1.

(14) Zevalkink, A. et al. A practical field guide to thermoelectrics: Fundamentals, synthesis, and characterization. *Applied Physics Reviews* **2018**, *5*, 021303.

(15) Vining, C. B.; Laskow, W.; Hanson, J. O.; Van der Beck, R. R.; Gorsuch, P. D. Thermoelectric properties of pressure-sintered $Si_{0.8}Ge_{0.2}$ thermoelectric alloys. *Journal of applied physics* **1991**, *69*, 4333–4340.

(16) Wood, M.; Kuo, J. J.; Imasato, K.; Snyder, G. J. Improvement of Low-Temperature zT in a Mg_3Sb_2–Mg_3Bi_2 Solid Solution via Mg-Vapor Annealing. *Advanced Materials* **2019**, 1902337.

(17) Bachmann, M.; Czerner, M.; Heiliger, C. Ineffectiveness of energy filtering at grain boundaries for thermoelectric materials. *Physical Review B* **2012**, *86*, 115320.

(18) Pei, Y.; Lensch-Falk, J.; Toberer, E. S.; Medlin, D. L.; Snyder, G. J. High thermoelectric performance in PbTe due to large nanoscale Ag_2Te precipitates and La doping. *Advanced Functional Materials* **2011**, *21*, 241–249.

(19) Kuo, J. J.; Aydemir, U.; Pöhls, J.-H.; Zhou, F.; Yu, G.; Faghaninia, A.; Ricci, F.; White, M. A.; Rignanese, G.-M.; Hautier, G.; Jain, A.; Snyder, G. J. Origins of ultralow thermal conductivity in 1-2-1-4 quaternary selenides. *Journal of Materials Chemistry A* **2019**, *7*, 2589–2596.

(20) Ashcroft, N. W.; Mermin, N. D. Solid state physics (saunders college, philadelphia, 1976). *Appendix N* **2010**,

(21) Kuo, J. J.; Yu, Y.; Kang, S. D.; Cojocaru-Mirédin, O.; Wuttig, M.; Snyder, G. J. Mg Deficiency in Grain Boundaries of n-Type Mg_3Sb_2 Identified by Atom Probe Tomography. *Advanced Materials Interfaces* **2019**, 1900429.

(22) Cantwell, P. R.; Tang, M.; Dillon, S. J.; Luo, J.; Rohrer, G. S.; Harmer, M. P. Grain boundary complexions. *Acta Materialia* **2014**, *62*, 1–48.

(23) Bergman, D. J.; Levy, O. Thermoelectric properties of a composite medium. *Journal of Applied Physics* **1991**, *70*, 6821–6833.

(24) Nan, C.-W.; Birringer, R.; Clarke, D. R.; Gleiter, H. Effective thermal conductivity of particulate composites with interfacial thermal resistance. *Journal of Applied Physics* **1997**, *81*, 6692–6699.

(25) Wood, M.; Kuo, J. J.; Imasato, K.; Snyder, G. J. Improvement of Low-Temperature zT in a Mg_3Sb_2–Mg_3Bi_2 Solid Solution via Mg-Vapor Annealing. *Advanced Materials* **2019**, 1902337.

(26) Androulakis, J.; Todorov, I.; Chung, D.-Y.; Ballikaya, S.; Wang, G.; Uher, C.; Kanatzidis, M. Thermoelectric enhancement in PbTe with K or Na codoping from tuning the interaction of the light-and heavy-hole valence bands. *Physical Review B* **2010**, *82*, 115209.

(27) Slade, T. J.; Grovogui, J. A.; Kuo, J. J.; Anad, S.; Bailey, T. P.; Wood, M.; Uher, C.; Snyder, G. J.; Dravid, V. P.; Kanatzidis, M. G. *in Preparation* **2019**,

(28) Zhao, L.-D.; Lo, S.-H.; Zhang, Y.; Sun, H.; Tan, G.; Uher, C.; Wolverton, C.; Dravid, V. P.; Kanatzidis, M. G. Ultralow thermal conductivity and high thermoelectric figure of merit in SnSe crystals. *Nature* **2014**, *508*, 373.

(29) Lee, Y. K.; Luo, Z.; Cho, S. P.; Kanatzidis, M. G.; Chung, I. Surface oxide removal for polycrystalline SnSe reveals near-single-crystal thermoelectric performance. *Joule* **2019**, *3*, 719–731.

(30) Zhou, Z.; Agne, M. T.; Zhang, Q.; Wan, S.; Song, Q.; Xu, Q.; Lu, X.; Gu, S.; Fan, Y.; Jiang, W.; Snyder, G. J.; Wang, L. Microstructure and composition engineering Yb single-filled CoSb3 for high thermoelectric and mechanical performances. *Journal of Materiomics* **2019**,

(31) Hu, L.; Liu, X.; Xie, H.; Shen, J.; Zhu, T.; Zhao, X. Improving thermoelectric properties of n-type bismuth–telluride-based alloys by deformation-induced lattice defects and texture enhancement. *Acta Materialia* **2012**, *60*, 4431–4437.

(32) Zhao, L.-D.; Lo, S.-H.; Zhang, Y.; Sun, H.; Tan, G.; Uher, C.; Wolverton, C.; Dravid, V. P.; Kanatzidis, M. G. Ultralow thermal conductivity and high thermoelectric figure of merit in SnSe crystals. *Nature* **2014**, *508*, 373.

(33) Wang, S.; Hui, S.; Peng, K.; Bailey, T. P.; Zhou, X.; Tang, X.; Uher, C. Grain boundary scattering effects on mobilities in p-type polycrystalline SnSe. *Journal of Materials Chemistry C* **2017**, *5*, 10191–10200.

(34) Yu, J.; Yue, A.; Stafsudd, O. Growth and electronic properties of the SnSe semiconductor. *Journal of Crystal Growth* **1981**, *54*, 248 – 252.

(35) Albers, W.; Haas, C.; Ober, H.; Schodder, G.; Wasscher, J. Preparation and properties of mixed crystals SnS(1-x)Sex. *Journal of Physics and Chemistry of Solids* **1962**, *23*, 215 – 220.

(36) Chen, S.; Cai, K.; Zhao, W. The effect of Te doping on the electronic structure and thermoelectric properties of SnSe. *Physica B: Condensed Matter* **2012**, *407*, 4154–4159.

(37) Sassi, S.; Candolfi, C.; Vaney, J.-B.; Ohorodniichuk, V.; Masschelein, P.; Dauscher, A.; Lenoir, B. Assessment of the thermoelectric performance of polycrystalline p-type SnSe. *Applied Physics Letters* **2014**, *104*, 212105.

(38) Zhu, T.; Xu, Z.; He, J.; Shen, J.; Zhu, S.; Hu, L.; Tritt, T. M.; Zhao, X. Hot deformation induced bulk nanostructuring of unidirectionally grown p-type (Bi, Sb) 2 Te 3 thermoelectric materials. *Journal of Materials Chemistry A* **2013**, *1*, 11589–11594.

(39) Zhao, L.; Zhang, B.-P.; Li, J.-F.; Zhang, H.; Liu, W. Enhanced thermoelectric and

mechanical properties in textured n-type Bi2Te3 prepared by spark plasma sintering. *Solid State Sciences* **2008**, *10*, 651–658.

(40) Son, J.-H.; Oh, M.-W.; Kim, B.-S.; Park, S.-D. Optimization of thermoelectric properties of n-type Bi 2 (Te, Se) 3 with optimizing ball milling time. *Rare Metals* **2018**, *37*, 351–359.

(41) LaLonde, A. D.; Ikeda, T.; Snyder, G. J. Rapid consolidation of powdered materials by induction hot pressing. *Review of Scientific Instruments* **2011**, *82*, 025104.

(42) Borup, K. A.; De Boor, J.; Wang, H.; Drymiotis, F.; Gascoin, F.; Shi, X.; Chen, L.; Fedorov, M. I.; Müller, E.; Iversen, B. B.; Snyder, G. J. Measuring thermoelectric transport properties of materials. *Energy & Environmental Science* **2015**, *8*, 423–435.

(43) Iwanaga, S.; Toberer, E. S.; LaLonde, A.; Snyder, G. J. A high temperature apparatus for measurement of the Seebeck coefficient. *Review of Scientific Instruments* **2011**, *82*, 063905.

(44) Agne, M. T.; Hanus, R.; Snyder, G. J. Minimum thermal conductivity in the context of diffuson-mediated thermal transport. *Energy & Environmental Science* **2018**, *11*, 609–616.